

RESEARCH ARTICLE

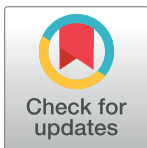
Positive effect of an electrolyzed reduced water on gut permeability, fecal microbiota and liver in an animal model of Parkinson's disease

Laura Bordoni¹, Rosita Gabbianelli¹, Donatella Fedeli¹, Dennis Fiorini², Ina Bergheim³, Cheng Jun Jin⁴, Lisa Marinelli⁵, Antonio Di Stefano⁵, Cinzia Nasuti⁶*

1 School of Pharmacy, Molecular Biology Unit, University of Camerino, Camerino, Italy, **2** School of Science and Technology, Chemistry Unit, University of Camerino, Camerino, Italy, **3** Department of Nutritional Sciences, RF Molecular Nutritional Science, University of Vienna, Vienna, Austria, **4** Institute of Nutritional Sciences, SD Model Systems of Molecular Nutrition, Friedrich-Schiller-University, Jena, Germany, **5** Department of Pharmacy, University of "G. D'Annunzio", Chieti, Italy, **6** School of Pharmacy, Pharmacology Unit, University of Camerino, Camerino, Italy

☉ These authors contributed equally to this work.

* cinzianasuti@unicam.it



OPEN ACCESS

Citation: Bordoni L, Gabbianelli R, Fedeli D, Fiorini D, Bergheim I, Jin CJ, et al. (2019) Positive effect of an electrolyzed reduced water on gut permeability, fecal microbiota and liver in an animal model of Parkinson's disease. PLoS ONE 14(10): e0223238. <https://doi.org/10.1371/journal.pone.0223238>

Editor: Brenda A. Wilson, University of Illinois at Urbana-Champaign, UNITED STATES

Received: January 7, 2019

Accepted: September 17, 2019

Published: October 10, 2019

Copyright: © 2019 Bordoni et al. This is an open access article distributed under the terms of the [Creative Commons Attribution License](https://creativecommons.org/licenses/by/4.0/), which permits unrestricted use, distribution, and reproduction in any medium, provided the original author and source are credited.

Data Availability Statement: All relevant data are within the paper and its Supporting Information files.

Funding: The authors received no specific funding for this work.

Competing interests: The authors have declared that no competing interests exist.

Abstract

There is growing awareness within the scientific community of the strong connection between the inflammation in the intestine and the pathogenesis of Parkinson's disease (PD). In previous studies we developed a PD animal model exposing pup rats to permethrin (PERM) pesticide. Here, we intended to explore whether in our animal model there were changes in gut permeability, fecal microbiota and hepatic injury. Moreover, we tested if the co-treatment with an electrolyzed reduced (ERW) was effective to protect against alterations induced by PERM. Rats (from postnatal day 6 to 21) were gavaged daily with PERM, PERM+ERW or vehicle and gut, liver and feces were analyzed in 2-months-old rats. Increased gut permeability, measured by FITC-dextran assay, was detected in PERM group compared to control and PERM+ERW groups. In duodenum and ileum, concentration of occludin was higher in control group than those measured in PERM group, whereas only in duodenum ZO-1 was higher in control than those measured in PERM and PERM+ERW groups. Number of inflammatory foci and neutrophils as well as iNOS protein levels were higher in livers of PERM-treated rats than in those of PERM+ERW and control rats. Fecal microbiota analysis revealed that *Lachnospira* was less abundant and *Defluviitaleaceae* more abundant in the PERM group, whereas the co-treatment with ERW was protective against PERM treatment since the abundances in *Lachnospira* and *Defluviitaleaceae* were similar to those in the control group. Higher abundances of butyrate-producing bacteria such as *Blautia*, *U.m. of Lachnospiraceae* family, *U.m. of Ruminococcaceae* family, *Papillibacter*, *Roseburia*, *Intestinimonas*, *Shuttleworthia* together with higher butyric acid levels were detected in PERM+ERW group compared to the other groups. In conclusion, the PD animal model showed increased intestinal permeability together with hepatic inflammation

correlated with altered gut microbiota. The positive effects of ERW co-treatment observed in gut, liver and brain of rats were linked to changes on gut microbiota.

Introduction

Permethrin (PERM) is a pesticide belonging to the pyrethroid family that has been used to induce Parkinson's disease (PD) in an animal model. In our previous studies, neonatal rats treated daily per o.s. for 2 weeks with permethrin (34 mg/kg body weight) developed the three pathological hallmarks of PD: namely loss of dopaminergic neurons in the substantia nigra, increase of free and aggregated alpha-synuclein protein levels reminiscent of Lewy bodies and motor and non-motor symptoms correlated with PD [1], [2], [3], [4]. Successively, we observed that the co-treatment with electrochemically reduced water (ERW), a hydrogen-rich water buffered to pH 7.4, was able to protect against damage on dopaminergic neurons induced by permethrin treatment [5]. The ERW is a water supersaturated with active hydrogen produced near the cathode during electrolysis of water. It is a functional drinking water with highly dissolved molecular hydrogen (0.4–0.9 ppm) and extremely negative oxidative redox potential (ORP) values (-300 mV) that possesses reactive oxygen species (ROS)-scavenging activity conferred by the effect of dissolved H₂ [6].

In recent years, it has become clear that PD is associated with a number of gastrointestinal symptoms such as constipation originating from functional and structural changes in the gut and its enteric nervous system. These disturbances happen years before the development of motor symptoms and diagnosis of PD and may therefore provide important insights into the origin and development of the disease. There is accumulating evidence that the origin of the disease may lie in the gut with possible involvement of misfolded alpha-synuclein deposits observed in the enteric nervous system. Furthermore, alterations of gut microbiota composition, local inflammation and increased gut permeability have been shown in PD patients. Environmental factors such as exposure to pesticides seem to play a key role to initiate the pathophysiological cascade in PD. One proposed pathway is the disruption of gut microbiome composition and subsequent development of intestinal inflammation with retrograde ascension up the vagus nerve to reach the central nervous system [7], [8], [9]. It has been postulated that the enteric nervous system (ENS) is affected early during the progression of PD even before the substantia nigra, therefore supporting a key role for the ENS in the initiation and spreading of PD pathological process, although this hypothesis remains currently controversial.

Recent studies conducted in PD patients have demonstrated a shift of microbiota composition to a proinflammatory state related with higher lipopolysaccharide (LPS) levels [10]. Moreover, lower serum levels of LPS-binding protein (LBP) were found in PD patients which is indicating higher systemic LPS exposure [11]. The gut dysbiosis induces overstimulation of the innate immune system via TLR signalling and provokes local and systemic inflammation triggering the development of alpha-synuclein pathology [12], [13].

In the light of these premises, in this study, we intended to explore whether in our PD animal model there were changes in gut permeability, fecal microbiota composition and histological hallmarks of hepatic injury. Moreover, we tested if the co-treatment with ERW was effective to counterbalance gut alterations induced by PERM pesticide in the PD animal model.

Materials and methods

The study was carried out in strict accordance with the European Guidelines (Directive 2010/63/EU) for the Care and Use of Laboratory Animals. The protocol was approved by the Italian Ministry of Health (Protocol Number: 393/2016-PR). All efforts were made to minimize suffering.

Materials

Technical grade (75:25, trans:cis; 94% purity) 3-phenoxybenzyl-(1R,S)-cis,trans-3-(2,2-dichlorovinyl)-2,2-dimethylcyclopropanecarboxyl-ate, PERM (PubChem CID: 40326) were generously donated by Dr. A. Stefanini of ACTIVA (Milan, Italy). Corn oil, citric acid, fluorescein isothiocyanate—dextran 4 kDa (FITC-dextran), 3,3',5,5'-tetramethylbenzidine, hexadecyltrimethylammonium bromide, naphthol ASD-chloroacetate esterase kit were obtained from Sigma (Milan, Italy). 3,3'-diaminobenzidine (DAB) was purchased from DAKO (Hamburg, Germany). Periodic acid (1%), protease mixture and BSA were purchased from Carl Roth (Karlsruhe, Germany). Alcian blue 8GS was purchased from Serva (Heidelberg, Germany).

Animals and treatments

Male and female Wistar rats aged about 90 days weighing 250–270 g were obtained from Charles River (Calco, LC, Italy). Animals were housed in a room with artificial 12:12 h light/dark cycle (lights off at 8:00 a.m.), at constant temperature ($21\pm 5^\circ\text{C}$) and humidity (45–55%). Food and water were always available in the home cages. Male rat pups born in our laboratory from primiparous dams were assigned to three treatment groups ($n = 20$ PERM-treated rats, $n = 18$ controls and $n = 20$ PERM+ERW-treated rats) so that each group contained no more than 3 pups from any litter. At the time of weaning, rats were housed in single cages to avoid coprophagic behavior that leads to a confluence of the microbial populations among cage mates. The first group was treated once daily by gavage with PERM (34 mg/4 mL/kg body weight) from postnatal day (PND) 6 to PND 21, whereas the second group (control) was treated with the vehicle (corn oil 4 mL/kg body weight) on a similar schedule. PERM was prepared by dissolving the substance in the corn oil as previously described [14].

A third group was gavaged once a day with PERM (34 mg/4 mL/kg body weight) and co-treated twice a day (early morning and late afternoon) with ERW (10 mL/kg body weight) from PND 6 to PND 21. ERW was produced by a water ionizer and buffered with citric acid at a pH = 7.4 before use. On PND 60, animals were divided in two batches: one was submitted to *in vivo* intestinal permeability assay and the second was sacrificed by CO₂ asphyxiation and the tissues were submitted to analysis.

Preparation of electrolyzed reduced water

ERW was produced by a continuously electrolyzing device (Chanson Revolution 9 plates, Taiwan), wherein tap water is the water source. The device is composed of two units, a micro-carbon cartridge unit for removal of contaminants from tap water and an electrolysis unit that acts on the purified water. The latter passed through a micro-carbon cartridge unit and flows into the electrolysis unit, which is composed of platinum-coated electrode plates, separated by semi-permeable membranes and the water is electrolyzed while passing through the gaps between the electrodes. ERW is a functional drinking water characterized by a high pH (around 9.5–10), a low amount of dissolved oxygen, a low redox potential (ORP = -300 mV) and a high concentration of dissolved H₂ (0.4–0.9 ppm) compared with tap water (pH = 7.4,

ORP = +300 mV and H_2 = 0 ppm) that confers antioxidant activity to the water as reported by other studies [15], [16].

In vivo intestinal permeability assay

A first batch of rats, overnight fasted, from control (n = 8), PERM-treated (n = 10) and PERM+ERW-treated (n = 10) groups was assayed for gut permeability with FITC-dextran on PND 60. The low-molecular-weight fluorescent marker FITC-dextran powder was dissolved in pure water to a concentration of 100 mg/mL. Induction of anesthesia was achieved with 5% [isoflurane](#) in oxygen that the animals were breathing spontaneously through a gas anesthesia mask. The first blood sample was collected, from the tail of anesthetized rats (5% isoflurane), immediately prior to administration of FITC-dextran, as a negative control for plasma background fluorescence. The rats were then orally dosed with FITC-dextran solution (500 mg/kg body weight). Two hours after dosage, animals were anesthetized and blood was collected from the tail directly into tubes containing sodium heparin (5 μ L). Blood samples were immediately centrifuged (2,000 g force, 5 min) to collect plasma that was diluted 3:1 in PBS. A calibration curve for FITC-dextran in plasma was built and fluorescence intensities of samples were measured by spectrofluorometer Hitachi F-4500 using 485 and 528 nm as excitation and emission wavelengths, respectively.

Dopamine assessment in striatum nucleus

Tissues derived from the rat striatum were homogenized with 500 μ L of 1N perchloric acid solution containing 0.02% w/v sodium metabisulphite and 0.05% w/v disodium ethylenediaminetetraacetate (Na₂EDTA). Samples were centrifugated at 4500 x g for 20 min at 4°C. The obtained supernatants were filtered using 0.45 μ m filters, collected into vials and stored on ice until analysis. 10 μ L of the filtrate was analyzed by HPLC (Rheodyne 7295 injector and Antec Leyden Decade II detector) as reported in Bordoni et al. [3]. Final values were expressed as ng/mg tissue.

Histological and immunohistochemical stainings

From a second batch of control (n = 10), PERM-treated (n = 10) and PERM+ERW-treated (n = 10) rats, fecal pellets were freshly collected on PND 60, and stored at -80°C until analysis to quantify bacterial population and short-chain fatty acids (SCFA). On the same day, animals were killed by CO₂ asphyxiation. Samples of liver and intestine (duodenum, ileum and colon) were excised, washed briefly with phosphate-buffered saline (pH 7.4), fixed in 10% buffered formalin for 48 h and embedded in paraffin. The remaining tissues were frozen in liquid nitrogen and stored at -80°C.

Paraffin embedded liver tissue was cut (4 μ m), deparaffinized and stained with hematoxylin and eosin. Tissue sections were scored as described by Kleinert et al. [17]. Using a microscope (Leica, Wetzlar, Germany), number of neutrophils in liver sections was assessed by staining liver sections with chloroacetate esterase (naphthol ASD-chloroacetate esterase kit, Sigma-Aldrich) as previously detailed [18]. For detection of iNOS protein in liver tissue, liver sections were treated as previously described in detail [18]. In brief, sections were incubated with a polyclonal antibody against iNOS (dilution 1: 2250; Thermo Fischer Scientific, Waltham USA) overnight followed by an incubation with a secondary peroxidase-linked antibody and diaminobenzidine (Peroxidase Envision Kit, DAKO, Hamburg, Germany). The extent of staining in tissue sections was defined as percentage of the field area within the default color range determined by the software using an image acquisition and analysis system incorporated in the

microscope (Leica DM4000 B LED, Germany). To determine means, data from 8 fields of each tissue section were used (200 x magnification).

For tissue-specific localization of tight junction proteins in sections of duodenum, ileum and colon (4 μ M) immunohistochemical staining of zonula occludens 1 (ZO-1) and occludin was performed as previously reported [18]. In brief, sections were incubated with a polyclonal antibody (anti-ZO-1 or anti-occludin both Life Technologies, Darmstadt, Germany) overnight. Sections were then incubated with a secondary peroxidase-linked antibody and diaminobenzidine (Peroxidase Envision Kit, DAKO, Hamburg, Germany). The extent of staining in tissue sections was determined as detailed above using 8 fields of each tissue section to determine means (400 x magnification).

To assess number of mucus-producing Goblet cells in duodenum, ileum and colon tissue sections were stained with Alcian blue/periodic acid-Schiff as previously described [19]. Number of Goblet cells were counted in 10 microscopic fields (400 x magnification) and shown as means.

Measurement of liver myeloperoxidase (MPO) activity

MPO activity was measured photometrically employing 3,3',5,5'-tetramethylbenzidine as substrate as detailed before by us and others [20], [21].

SCFA in feces

Levels of acetic, propionic, and butyric acids were detected in feces of rats at PND 60. Ten feces samples for each rat group (one feces sample for each rat) were analyzed by headspace solid-phase microextraction coupled to gas-chromatography equipped with flame ionization detection as previously reported [22]. Triplicates of each homogenized sample were analyzed and results were expressed as μ mol/g feces.

Fecal microbiota analyses

Fecal samples collected at PND 60 from control (n = 10), PERM-treated (n = 10) and PERM +ERW-treated (n = 10) groups were evaluated using 16S rRNA gene sequencing to determine the composition of the fecal bacterial populations.

Partial 16S rRNA gene sequences were amplified from extracted DNA using primer pair Probio_Uni and /Probio_Rev, which target the V3 region of the 16S rRNA gene sequence [23]. 16S rRNA gene amplification and amplicon checks were carried out as previously described [23]. 16S rRNA gene sequencing was performed using a MiSeq (Illumina) at the DNA sequencing facility of GenProbio srl (www.genprobio.com) according to the protocol previously reported [23]. Following sequencing, the obtained individual sequence reads were filtered by the Illumina software to remove low quality and polyclonal sequences. All Illumina quality-approved, trimmed and filtered data were exported as .fastq files. The .fastq files were processed using a custom script based on the QIIME software suite [24]. Paired-end reads pairs were assembled to reconstruct the complete Probio_Uni / Probio_Rev amplicons. Quality control retained sequences with a length between 140 and 400 bp and mean sequence quality score >20 while sequences with homopolymers >7 bp and mismatched primers were omitted. In order to calculate downstream diversity measures (alpha and beta diversity indices, Unifrac analysis), 16S rRNA Operational Taxonomic Units (OTUs) were defined at \geq 97% sequence homology using uclust [25]. All reads were classified to the lowest possible taxonomic rank using QIIME [24] and a reference dataset from the SILVA database [26]. Biodiversity of the samples (alpha-diversity) were calculated with Chao1 and Shannon indexes measured at 47746 reads [27]. Similarities between samples (beta-diversity) were calculated by

unweighted uniFrac [28]. The range of similarities is calculated between the values 0 and 1. PCoA representations of beta-diversity were performed using QIIME [24]. Hierarchical clusterings were performed with TMeV 4.8.1 (<http://www.tm4.org>) using Pearson correlation.

Statistical analysis

Statistical analysis was carried out using the program Statistica 8.0 (StatSoft Italy Srl, Vigonza, Italy, 2007). Data were analysed using an one-way ANOVA followed by post hoc Newman-Keuls test. Since data were not normally distributed, a non-parametric Kruskal-Wallis test was employed. Differences were considered significant at a P-value of 0.05.

Results

Evaluation of intestinal permeability with FITC-dextran

At PND 60, a first batch of control, PERM-treated and PERM+ERW-treated rats was tested for FITC-dextran concentration in plasma in order to assess intestinal permeability. One way ANOVA revealed significant differences ($F_{(2,25)} = 3.41$, $P < 0.05$) in FITC-dextran concentration among the three groups (Fig 1A). Post hoc comparisons revealed a significant increased intestinal permeability in PERM-treated rats compared to the control group ($P < 0.05$), whereas no difference was observed between PERM+ERW-treated rats and control ones ($P > 0.05$). These results showed that early life exposure to PERM, in rats aged 60 days, altered permeability to FITC-dextran and the co-treatment with ERW improved intestinal barrier integrity.

Dopamine levels in striatum nucleus

At PND 60, dopamine levels were measured in striatum nucleus of control, PERM-treated and PERM+ERW-treated rats. One way ANOVA revealed significant differences ($F_{(2,15)} = 14.94$, $P < 0.01$) in dopamine levels among the three groups (Fig 1B). Post hoc comparisons revealed a significant decreased dopamine levels in striatum of PERM-treated rats compared to the control group ($P < 0.01$) as previously reported [1], [2], [3], [14]. The co-treatment with ERW increased the dopamine levels that were similar to those of control rats ($P > 0.05$). The results suggested that early life exposure to PERM, in rats aged 60 days, altered dopamine levels in striatum and the co-treatment with ERW could protect against the neurodegeneration.

Histological findings in liver and MPO activity

While rats treated with PERM displayed significantly more signs of hepatic inflammation, e.g. inflammatory foci, than animals treated with PERM+ERW or control animals ($P < 0.05$ for both), the nonalcoholic fatty liver disease activity score (NAS) between control and PERM+ERW-treated rats was similar. In line with these findings, the number of neutrophils was also higher in livers of PERM-treated animals than in those of controls and PERM+ERW-treated rats ($P < 0.05$ for both). However, as data varied considerable within groups, activity of MPO in liver tissue did not differ among groups ($P > 0.05$). Data are reported in Table 1 and Fig 2A.

Immunohistochemical findings in duodenum, ileum and colon and iNOS protein levels in liver tissue

To further delineate if the increased permeability of FITC-dextran was related to a loss of tight junction proteins in the small or large intestine, protein levels of ZO-1 and occludin were determined in duodenum, ileum and colon (Fig 2B and Table 1). Occludin protein levels were significantly lower in PERM-treated rats when compared to controls and did not differ from those of PERM+ERW-treated animals ($P > 0.05$) in duodenum. Moreover, ZO-1 protein

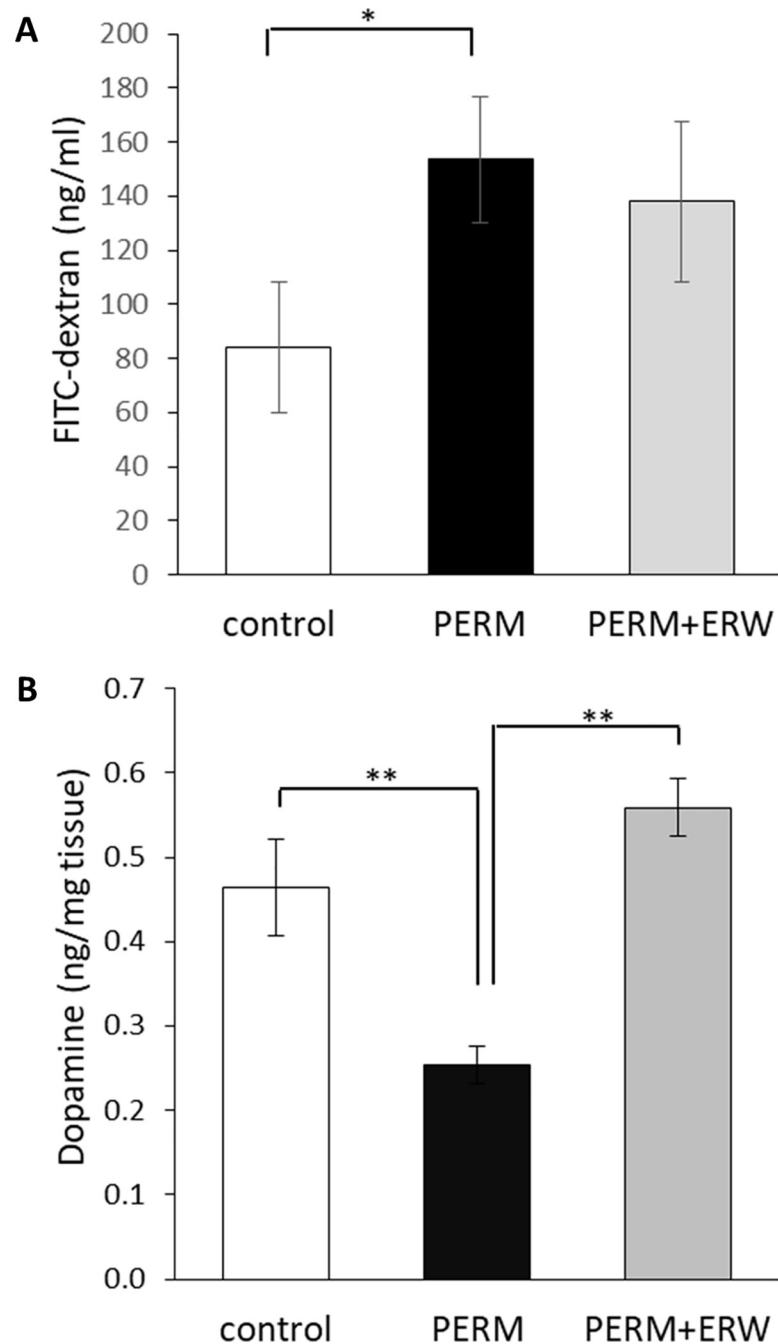


Fig 1. Plasma FITC-dextran concentrations (ng/mL) (A) and striatum dopamine levels (B) in 2-months-old rats treated in early life with vehicle (control), permethrin (PERM) or permethrin+electrolyzed reduced water (PERM+ERW). The increase of intestinal permeability and the decrease of striatum dopamine levels in the PERM group were improved by co-treatment with ERW. All data are expressed as means \pm SEM. Group sizes in A: control (n = 8), PERM (n = 10) and PERM+ERW (n = 10), *P<0.05. Group sizes in B: n = 6 rats per group, **P<0.01.

<https://doi.org/10.1371/journal.pone.0223238.g001>

concentration was significantly lower in duodenum of PERM-treated rats and PERM+ERW-treated animals when compared to controls. In ileum of PERM-treated rats protein, levels of occludin were significantly lower than in all other groups (P<0.05 for both) while protein

Table 1. Scores measured in liver (L), duodenum (D), ileum (I), colon (C) and feces (F) of 2-months-old rats treated in early life with vehicle (C), permethrin (PERM) or permethrin+electrolyzed reduced water (PERM+ERW).

		C	PERM	PERM+ERW	C vs PERM	PERM vs PERM+ERW	C vs PERM+ERW
L	Inflammation (NAS)	0.31±0.09	0.98±0.04	0.57±0.04	***	*	
	Neutrophils (n. per MF)	2.05±0.47	3.36±0.49	1.83±0.37	*	*	
	iNOS activity (% per MF)	3.56±0.35	6.77±0.55	2.34±0.37	*	***	
	MPO activity (A/mg protein)	2.8x10 ⁻³ ±3x10 ⁻⁴	6.5x10 ⁻³ ±3x10 ⁻³	2.7x10 ⁻³ ±2x10 ⁻⁴			
D	Occludin (% per MF)	8.59±0.91	5.11±0.82	5.85±0.84	*		
	ZO-1 (% per MF)	17.02±2.85	7.59±1.99	5.04±0.46	*		**
	Goblet cells (n. per MF)	0.03±3x10 ⁻³	0.03±3x10 ⁻³	0.03±1x10 ⁻³			
I	Occludin (n. per MF)	4.13±0.60	2.58±0.37	4.36±0.48	*	*	
	ZO-1 (% per MF)	4.93±1.26	2.62±0.61	3.82±0.93			
	Goblet cells (n. per MF)	0.07±8x10 ⁻³	0.07±4x10 ⁻³	0.06±7x10 ⁻³			
C	Occludin (% per MF)	2.39±0.23	2.35±0.30	2.45±0.29			
	ZO-1 (% per MF)	16.02±1.28	14.98±0.79	14.62±1.24			
	Goblet cells (n. per MF)	407±33.54	346±27.18	350±19.80			
F	Acetic acid (μmol/g)	126±8.39	106±8.14	121±11.82			
	Propionic acid (μmol/g)	12.83±1.43	16.81±1.42	15.45±1.87			
	Butyric acid (μmol/g)	9.85±1.38	13.61±1.06	14.87±1.65			*

All data are expressed as means ± SEM. Group sizes: C (n = 10), PERM (n = 10) and PERM+ERW (n = 10). MPO, myeloperoxidase; n, number of positive cells stained; A, absorbance; MF, microscopic field; NAS, non-alcoholic fatty liver disease activity score.

*P<0.05

**P<0.01

***P<0.001

<https://doi.org/10.1371/journal.pone.0223238.t001>

levels of ZO-1 were similar among groups in this part of the small intestine. Neither protein levels of ZO-1 nor occludin differed between groups in colon. Also, the number of goblet cells was similar among groups in all three parts of small and large intestine studied.

As it has been suggested before that an increased intestinal permeability and subsequently elevated translocation of bacterial endotoxin leads to an induction of iNOS in the liver [29], [18], protein levels of iNOS were determined in liver tissue (Fig 2A and Table 1). In line with the findings for liver histology but also for markers of intestinal permeability, iNOS protein levels were significantly higher in livers of PERM-treated rats than in those of PERM+ERW animals and controls. Levels of iNOS protein did not differ between PERM+ERW-treated rats and controls (P>0.05).

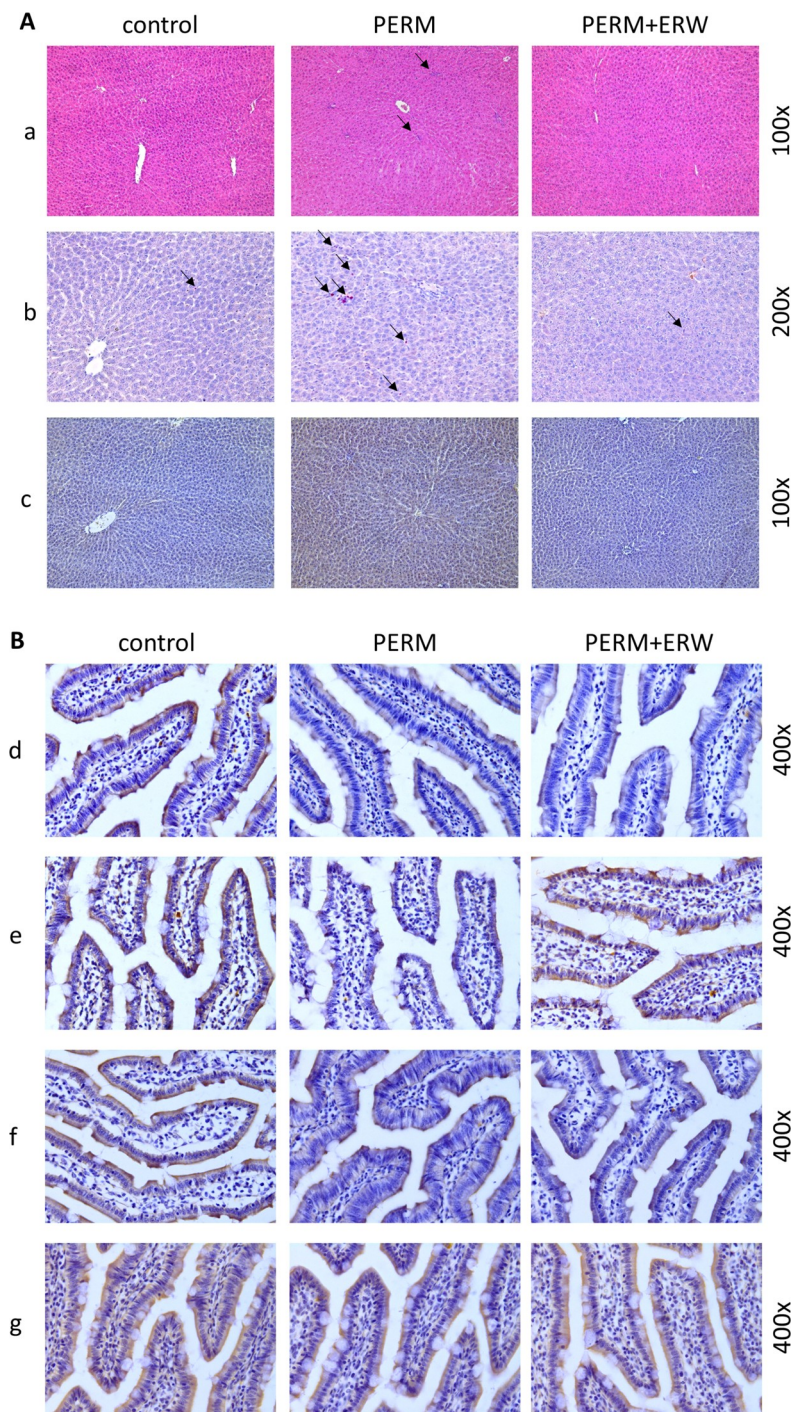


Fig 2. Representative stainings of liver (A) and intestinal (B) sections in 2-month-old rats treated in early life with vehicle (control), permethrin (PERM) or permethrin+electrolyzed reduced water (PERM+ERW) from left to right, respectively (100X, 200X and 400X magnification). In A: a) hematoxylin-eosin staining with clusters (aggregates) of inflammatory cells indicated by arrows; b) infiltration of activated neutrophils assessed by staining chloroacetate esterase. Arrows indicate neutrophils; c) immunohistochemical detection of iNOS expression. In B: immunohistochemical detection of occludin in d) duodenum and e) ileum; and ZO-1 in f) duodenum and g) ileum.

<https://doi.org/10.1371/journal.pone.0223238.g002>

Levels of SCFA in feces

Results revealed no significant difference ($F_{(2,27)} = 1.15$, $P > 0.05$; $F_{(2,27)} = 1.62$, $P > 0.05$) among control, PERM-treated and PERM+ERW-treated groups for acetic and propionic acid levels in the feces, as shown in Table 1. On the other hand, different levels of butyric acid levels ($F_{(2,27)} = 3.55$, $P < 0.05$) were measured among the three groups. Post hoc analysis revealed that butyric acid was significantly higher in PERM+ERW-treated group than in controls ($P = 0.041$). These results showed that co-treatment in early life with ERW may be able to increase the population of butyric acid producing bacteria.

Microbiota composition in feces

Thirty fecal samples collected at PND 60 were evaluated using 16S rRNA gene sequencing to determine the composition of the fecal bacterial populations in 10 control, 10 PERM-treated and 10 PERM+ERW-treated rats. To determine the bacterial community diversity in samples, we calculated Chao and Shannon indexes (Fig 3). Both indexes, which are calculated based on the number and distribution of OTUs, showed statistical differences among groups. The samples belonging to PERM+ERW-treated group showed higher Chao1 index compared to those of PERM-treated group ($P = 0.004$) and higher Shannon index compared with those of PERM-treated and control groups ($P = 0.016$ and $P = 0.045$, respectively).

Principal coordinates analysis (PCoA) showed a significant difference in bacterial composition between PERM and PERM+ERW groups. In fact, the subjects of the two groups formed distinct clusters, based on the first two principal component scores, which accounted for 41.63% and 11.88% of the total variations, respectively (Fig 4). On the contrary, there was substantial overlap between control and the other two groups, and most control samples were positioned in the middle of the PERM and PERM+ERW clusters.

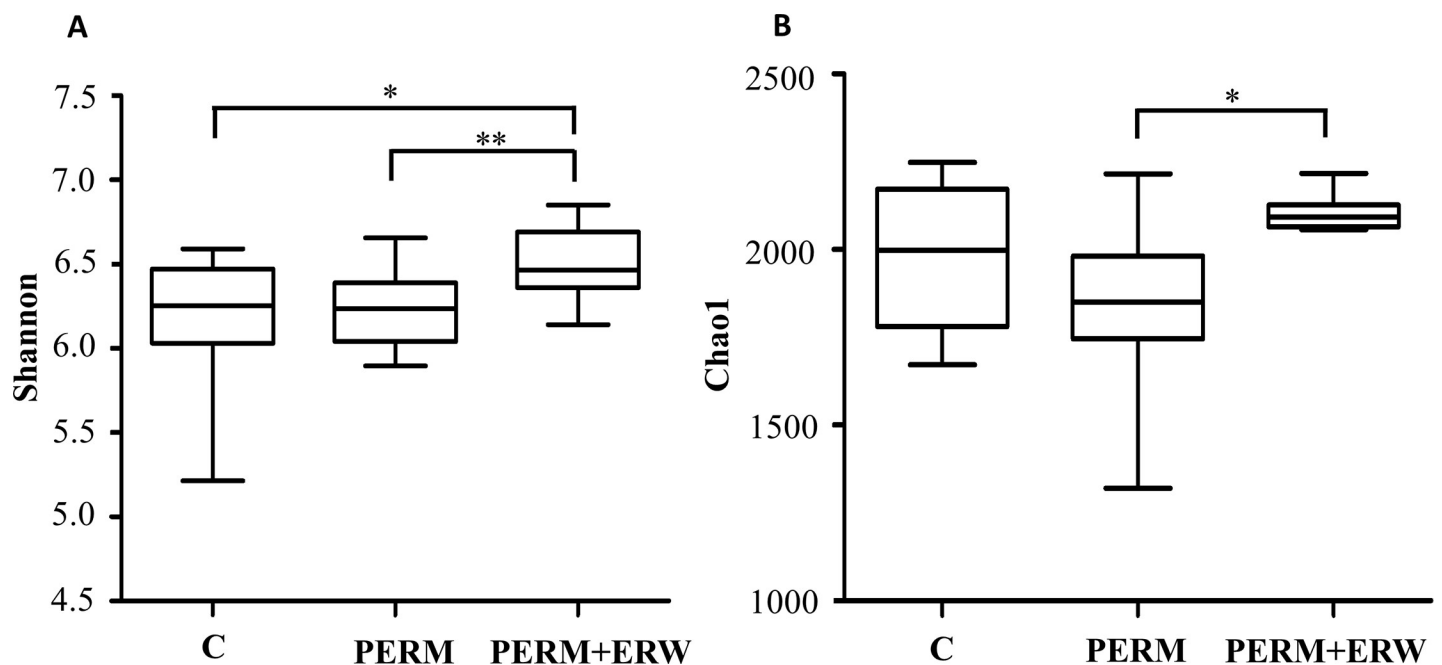


Fig 3. Significance of alpha diversity estimators in fecal microbiota of 2-month-old rats treated in early life with vehicle (C), permethrin (PERM) or permethrin +electrolyzed reduced water (PERM+ERW). Each group is made of n = 10 animals. * $P < 0.05$; ** $P < 0.01$.

<https://doi.org/10.1371/journal.pone.0223238.g003>

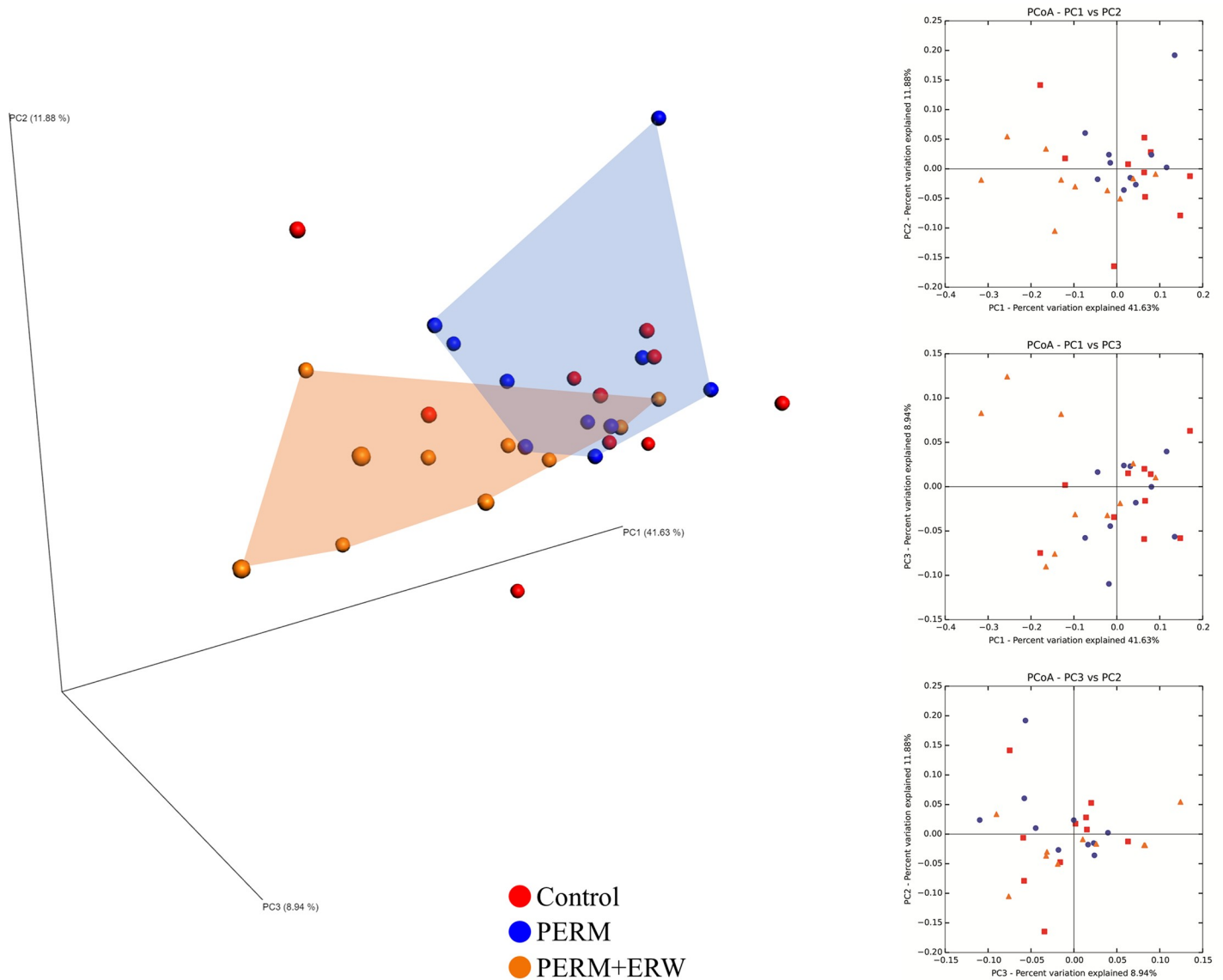


Fig 4. Comparison of variation in fecal microbiota of 2-month-old rats treated in early life with vehicle (Control), permethrin (PERM) or permethrin +electrolyzed reduced water (PERM+ERW). Principal coordinate plot of weighted UniFrac distances between fecal samples. Each dot represents a sample: red, Control; blu, PERM; orange, PERM+ERW.

<https://doi.org/10.1371/journal.pone.0223238.g004>

Looking at microbial abundance after early life treatment with vehicle, PERM or PERM +ERW, we observed differences among groups at the family and genus levels as shown in supplementary [S1 Table](#). Phyla *Firmicutes* and *Bacteroidetes* were the most abundant in all animals. In both control and PERM groups, *Bacteroidetes* were more abundant than in the PERM +ERW group ($P < 0.01$), whereas *Firmicutes* were more abundant in the PERM+ERW group ($P < 0.01$). Moreover, the latter exhibited higher abundances of phylum *Proteobacteria* compared to the other groups ($P < 0.05$) for the presence of higher percentage of genus *Desulfovibrio* belonging to this phylum.

A total of 57 genera identified from all samples are shown in detail in [S1 Table](#) and the heat-map exhibits the distribution of the top abundant genera among all samples ([S1 Fig](#)). The 6 most abundant genera, containing more than 85% of the total sequences, were *Prevotella*, *U.m.*

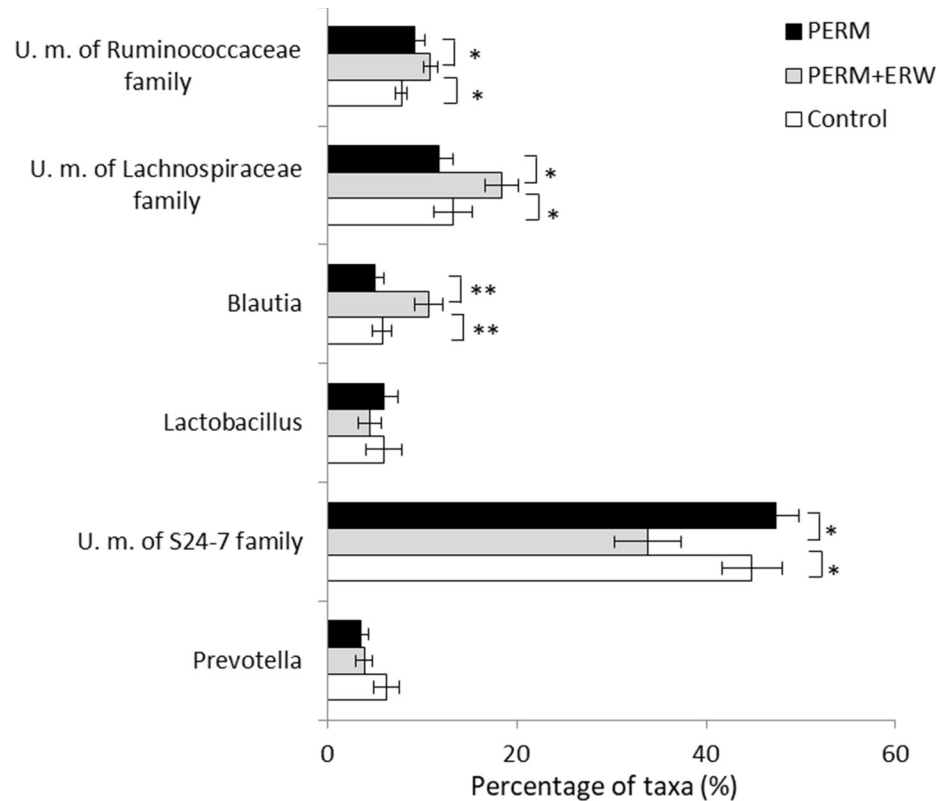


Fig 5. Relative abundance of 6 most predominant bacterial genera (relative abundance $\geq 85\%$ in sample) in fecal microbiota of 2-month-old rats treated in early life with vehicle (Control), permethrin (PERM) or permethrin +electrolyzed reduced water (PERM+ERW). All data are expressed as means \pm SEM. Each group is made of $n = 10$ animals. * $P < 0.05$; ** $P < 0.01$.

<https://doi.org/10.1371/journal.pone.0223238.g005>

of S24-7 family, *Lactobacillus*, *Blautia*, *U.m. of Lachnospiraceae* family and *U.m. of Ruminococcaceae* family. Of them, *U.m. of Prevotellaceae* family and *U.m. of S24-7* family were members of the phylum *Bacteroidetes*, whereas the other 4 genera belong to the phylum *Firmicutes*. Among the 6 most abundant genera, the fecal microbiota of PERM+ERW group exhibited significantly lower abundances of *U.m. of S24-7* family ($P < 0.05$) and higher abundances of *Blautia* ($P < 0.01$), *U.m. of Lachnospiraceae* family ($P < 0.05$) and *U.m. of Ruminococcaceae* family ($P < 0.01$) than the other two groups as showed in Fig 5.

Among the other less abundant genera, differences between control and PERM groups were observed for *Lachnospira* resulting less abundant ($P < 0.05$) and *Defluviitaleaceae* resulting more abundant in the PERM group ($P < 0.05$), whereas the co-treatment with ERW was protective against PERM treatment since that the abundance in *Lachnospira* ($P > 0.05$ vs control group) and *Defluviitaleaceae* ($P > 0.05$) was similar than in the control group. Other potentially important butyrate producers were increased in the PERM+ERW group compared to the other two groups, such as *Roseburia* ($P < 0.01$ vs PERM group), *Oscillibacter* ($P < 0.01$ vs PERM group), *Intestinimonas* ($P < 0.05$ vs PERM group), *Papillibacter* ($P < 0.01$ vs PERM group, $P < 0.05$ vs control group) and *Shuttleworthia* ($P < 0.05$ vs PERM group).

Discussion

ERW produced from tap water by electrolyzing device exhibits low dissolved oxygen, extremely high dissolved molecular hydrogen, and most importantly, shows ROS scavenging

activity and protective effects against oxidative damage as demonstrated in a MPTP mouse model of Parkinson's disease [30]. A clinical study shows that the negative ORP of ERW creates a gut environment by which protective microbiota, especially anaerobic bacteria, thrives allowing a protection against pathogenic bacteria in patients with irritable bowel syndrome [31].

In a preliminary study, we demonstrated that perinatal oral exposure to PERM pesticide could negatively affect the fecal microbiota and could be a crucial factor contributing to the development of PD in this animal model [22].

In this study, we attempted to further elucidate the effect of ERW co-treatment in the same animal model of PD focusing on intestinal permeability, fecal microbiota composition and histological hallmarks of hepatic injury measured 40 days after the last treatment (PND 60).

The main finding emerged from this study concerns the increased gut permeability, measured by FITC-dextran assay, in PERM group compared to control group. The fact that elevated permeability was not observed in PERM+ERW group indicated that ERW co-treatment was effective to protect the intestinal barrier against the damage induced by PERM. Since increased intestinal permeability often involves a disruption of the tight junction proteins, their expression in duodenum, ileum and colon was measured. In duodenum, a decrease of occludin and ZO-1 protein levels in PERM-treated rats when compared to controls was observed, whereas animals co-treated with ERW did not show an improvement. The protective effect of ERW co-treatment against PERM-induced intestinal permeability was observed in the ileum, where protein levels of occludin were higher than those measured in PERM-treated rats similarly to those of controls. Since defective mucus barrier resulting from depletion of goblet cells seems to be associated with increased intestinal permeability, we measured the number of goblet cells in the duodenum, ileum and colon. However, no significant differences were observed among groups in all three parts of small and large intestine.

Histological hallmarks of hepatic inflammation were investigated in the animals at PND 60. Inflammatory reactions in the liver often appear concurrently to a translocation of bacteria and their products across the leaky intestinal barrier to the liver. In line with the increased permeability of FITC-dextran, hepatic inflammation, number of neutrophils and iNOS protein levels were higher in livers of PERM-treated rats than in those of PERM+ERW animals and controls. The results, here obtained, allow us to postulate a first hypothesis: the ERW co-treatment in early life could protect intestinal barrier and then prevent liver damage. However, the intestinal barrier acts as a shield which can be modified by the gut microbiota and its metabolites such as the SCFA. In order to verify the hypothesis that the positive effects of ERW co-treatment observed in rats treated with PERM were linked to changes on gut microbiota, we firstly determined the levels of fecal SCFA and secondly the composition of the fecal bacterial populations. The significant increase of butyric acid levels measured in feces of PERM+ERW rats may explain in part the positive role played by ERW on gut microbiota. As demonstrated by many studies, the action of butyric acid extends beyond energy source for colonocytes, playing a role in the down regulation of the expression of pro-inflammatory mediators such as nitric oxide, interleukin-6, and interleukin-12 in intestinal macrophages [32], [33].

To evaluate PERM+ERW administration effects on gut microbial composition, we compared the relative abundance of the entire detected taxa in each group. Our investigation of alpha diversity, for quantifying the bacterial component and relative richness of a specific community, revealed an elevation of diversity estimators (Shannon and Chao indexes) in the PERM+ERW group compared to the PERM group suggesting that a rich diversity of gut microbiota may be related to the co-treatment with ERW. Hierarchical clustering and PCoA analysis of beta diversity was able to discriminate PERM samples from PERM+ERW samples,

whereas control samples were positioned in the middle of the PERM and PERM+ERW samples.

At the phylum level, in the PERM+ERW group, the proportion of *Firmicutes* increased and the proportion of *Bacteroidetes* decreased significantly ($P < 0.01$) compared with those of the other two groups. Moreover, *Proteobacteria* community, present at low levels in the control and PERM groups, were enriched in the PERM+ERW group ($P < 0.05$) for the presence of higher abundance of genus *Desulfovibrio* belonging to this phylum. At the genus level, differences between control and PERM groups were observed for *Lachnospira* resulting less abundant ($P < 0.05$) and *Defluviitaleaceae* resulting more abundant in the PERM group ($P < 0.05$), whereas the co-treatment with ERW was protective against PERM treatment since that the abundances in *Lachnospira* ($P > 0.05$) and *Defluviitaleaceae* ($P > 0.05$) were similar to those in the control group. We speculate that these two communities might be considered as specific biomarkers in our animal model of Parkinson's disease. Prior literature indicates that lower *Lachnospira* and higher *Defluviitaleaceae* abundances were reported in an animal model with indomethacin-induced enteropathy [34].

Other significant differences in microbiota composition were associated to ERW co-treatment: higher abundances of *Blautia* ($P < 0.01$ vs PERM and control group), *U.m. of Lachnospiraceae family* ($P < 0.05$ vs PERM and control group), *U.m. of Ruminococcaceae family* ($P < 0.01$ vs PERM and control group), *Papillibacter* ($P < 0.01$ vs PERM group, $P < 0.05$ vs control group) were found in PERM+ERW group. Moreover, higher abundances of *Roseburia* ($P < 0.01$), *Oscillibacter* ($P < 0.01$), *Intestinimonas* ($P < 0.05$) and *Shuttleworthia* ($P < 0.05$) were found in the fecal samples of PERM+ERW group compared to PERM group. Most of these bacteria are important butyrate producers and this result is consistent with the higher butyric acid levels measured in the fecal samples of PERM+ERW group. Among these bacteria, *Blautia*, *U.m. of Lachnospiraceae family*, *U.m. of Ruminococcaceae family*, *Papillibacter*, *Roseburia*, *Intestinimonas*, *Shuttleworthia* are Firmicutes members belonging to *Clostridium* and they are obligate anaerobes producing butyrate as major products from the fermentation of non-digestible carbohydrates in the colon [35]. Changes in the gut environment such as carbon source availability and hydrogen partial pressure have a major role in shaping the composition and activity of the bacterial community [36], [37]. The results, here obtained, allow us to hypothesize that the co-treatment with ERW, a drinking water rich in hydrogen, could favour the growth of anaerobes by lowering the redox potential in the intestinal lumen. Data in the literature can support this idea: ERW with negative ORP value between -300 and -400 mV is the optimum range favouring the growth of strict anaerobes in the gut [38], [39].

On the other hand, the co-treatment with ERW increased significantly the abundances of *Desulfovibrio*, a sulfate-reducer strict anaerobe that utilizes hydrogen as electron donor to produce hydrogen sulfide (H_2S). At excessive concentrations, sulfide exerts pro-inflammatory effects on the colonic mucosa whereas at lower concentrations is used as energy substrate by colonocytes [40]. Considering that rats were co-treated twice a day with 10 mL/kg of ERW, we must point out that higher dosage could negatively affect colonic epithelial barrier.

In conclusion, our animal model of permethrin-induced Parkinson's disease [1] showed increased intestinal permeability together with hepatic inflammation correlated with altered gut microbiota. The positive effects of ERW co-treatment observed in gut, liver and brain of rats were linked to changes on gut microbiota. This study demonstrates that the co-treatment with a functional drinking water, could create a gut environment favourable for the fermentation process producing butyric acid. Food-base therapy such as ERW drinking or/and a diet rich in natural sources of butyrate is a highly appealing approach that, if validated, may be used in conjunction with traditional pharmacological treatments to improve outcomes in patients with brain disorders.

Further studies in germ-free mice are needed to characterize the precise mechanism by which these microbes affect the host physiology.

Supporting information

S1 Fig. Changes in fecal microbiota of 2-month-old rats treated in early life with vehicle (Control), permethrin (PERM) or permethrin+electrolyzed reduced water (PERM+ERW).

The heat map shows the relative abundance of bacterial genera identified in each sample, the three groups (n = 10 rats per group) are separated by green lines. Hierarchical clustering was performed using Pearson correlation.

(TIF)

S1 Table. Relative abundance of bacterial genera in fecal microbiota. Relative abundance of bacterial genera in fecal microbiota of 2-months-old rats treated in early life with vehicle (C), permethrin (PERM) or permethrin+electrolyzed reduced water (PERM+ERW). All data are expressed as means \pm SEM. Group sizes: control (n = 10), PERM (n = 10) and PERM+ERW (n = 10). Significance was determined using Kruskal-Wallis (^a) or ANOVA (^b). *P<0.05; **P<0.01; ***P<0.001.

(PDF)

Acknowledgments

The authors would like to thank Dr. Ivan Dus who kindly provided the water ionizer (Chanson Revolution 9 plates, Nerò H₂O d.o.o., Sezana, Slovenia) and GenProbio s.r.l. who performed the microbiota analysis.

Author Contributions

Conceptualization: Rosita Gabbianelli, Cinzia Nasuti.

Data curation: Laura Bordoni, Donatella Fedeli, Dennis Fiorini, Ina Bergheim, Cheng Jun Jin, Lisa Marinelli, Antonio Di Stefano.

Formal analysis: Cheng Jun Jin, Lisa Marinelli, Antonio Di Stefano.

Investigation: Dennis Fiorini.

Methodology: Donatella Fedeli.

Project administration: Rosita Gabbianelli.

Supervision: Ina Bergheim, Cinzia Nasuti.

Writing – original draft: Cinzia Nasuti.

Writing – review & editing: Laura Bordoni.

References

1. Nasuti C, Brunori G, Eusepi P, Marinelli L, Ciccocioppo R, Gabbianelli R. Early life exposure to permethrin: a progressive animal model of Parkinson's disease. *J Pharmacol Toxicol Methods*. 2017; 83: 80–86. <https://doi.org/10.1016/j.vascn.2016.10.003> PMID: 27756609
2. Fedeli D, Montani M, Bordoni L, Galeazzi R, Nasuti C, Correia-S L, et al. In vivo and in silico studies to identify mechanisms associated with Nurr1 modulation following early life exposure to permethrin in rats. *Neuroscience*. 2017; 340: 411–423. <https://doi.org/10.1016/j.neuroscience.2016.10.071> PMID: 27826104

3. Bordoni L, Nasuti C, Di Stefano A, Marinelli L, Gabbianelli R. Epigenetic Memory of Early-Life Parental Perturbation: Dopamine Decrease and DNA Methylation Changes in Offspring. *Oxid Med Cell Longev*. 2019; 19: 1472623. <https://doi.org/10.1155/2019/1472623> PMID: 30915194
4. Bordoni L, Nasuti C, Fedeli D, Galeazzi R, Laudadio E, Massaccesi L, et al. Early impairment of epigenetic pattern in neurodegeneration: Additional mechanisms behind pyrethroid toxicity. *Exp Gerontol*. 2019; 124: 110629. <https://doi.org/10.1016/j.exger.2019.06.002> PMID: 31175960
5. Nasuti C, Fedeli D, Bordoni L, Montani M, Dus I, Gabbianelli R. Effect of electrolyzed reduced water in an animal model of Parkinson-like disease. In: 2nd European Summer School on Nutrigenomics. September 5–9, 2016, Camerino, Italy: Abstracts. *J Nutrigenet Nutrigenomics*. 2016; 9: 16. <https://doi.org/10.1159/000448866>
6. Hamasaki T, Harada G, Nakamichi N, Kabayama S, Teruya K, Fugetsu B, et al. Electrochemically reduced water exerts superior reactive oxygen species scavenging activity in HT1080 cells than the equivalent level of hydrogen-dissolved water. *PLoS One*. 2017; 12(2): e0171192. <https://doi.org/10.1371/journal.pone.0171192> PMID: 28182635
7. Rietdijk CD, Perez-Pardo P, Garssen J, van Wezel RJ, Kraneveld AD. Exploring Braak's Hypothesis of Parkinson's Disease. *Front Neurol*. 2017; 8: 37. <https://doi.org/10.3389/fneur.2017.00037> PMID: 28243222
8. Pan-Montojo F and Reichmann H. Considerations on the role of environmental toxins in idiopathic Parkinson's disease pathophysiology. *Transl Neurodegener*. 2014; 3: 10. <https://doi.org/10.1186/2047-9158-3-10> PMID: 24826210
9. Lema Tomé CM, Tyson T, Rey NL, Grathwohl S, Britschgi M, Brundin P. Inflammation and α -synuclein's prion-like behavior in Parkinson's disease—is there a link? *Mol Neurobiol*. 2013; 47(2): 561–574. <https://doi.org/10.1007/s12035-012-8267-8> PMID: 22544647
10. Keshavarzian A, Green SJ, Engen PA, Voigt RM, Naqib A, Forsyth CB, et al. Colonic bacterial composition in Parkinson's disease. *Mov Disord*. 2015; 30: 1351–1360. <https://doi.org/10.1002/mds.26307> PMID: 26179554
11. Hasegawa S, Goto S, Tsuji H, Okuno T, Asahara T, Nomoto K, et al. Intestinal dysbiosis and lowered serum lipopolysaccharide-binding protein in Parkinson's disease. *PLoS One*. 2015; 10: e0142164. <https://doi.org/10.1371/journal.pone.0142164> PMID: 26539989
12. Caputi V, Giron MC. Microbiome-Gut-Brain Axis and Toll-Like Receptors in Parkinson's Disease. *Int J Mol Sci*. 2018; 19(6):1689.
13. Perez-Pardo P, Dodiya HB, Engen PA, Forsyth CB, Huschens AM, Shaikh M, et al. Role of TLR4 in the gut-brain axis in Parkinson's disease: a translational study from men to mice. *Gut*. 2019; 68(5): 829–843. <https://doi.org/10.1136/gutjnl-2018-316844> PMID: 30554160
14. Nasuti C, Gabbianelli R, Falcioni ML, Di Stefano A, Sozio P, Cantalamessa F. Dopaminergic system modulation, behavioural changes, and oxidative stress after neonatal administration of pyrethroids. *Toxicology*. 2007; 229: 194–205. <https://doi.org/10.1016/j.tox.2006.10.015> PMID: 17140720
15. Ohsawa I, Ishikawa M, Takahashi K, Watanabe M, Nishimaki K, Yamagata K, et al. Hydrogen acts as a therapeutic antioxidant by selectively reducing cytotoxic oxygen radicals. *Nat Med*. 2007; 13: 688–694. <https://doi.org/10.1038/nm1577> PMID: 17486089
16. Hamasaki T, Nakamichi N, Teruya K, Shirahata S. Removal efficiency of radioactive cesium and iodine ions by a flow-type apparatus designed for electrochemically reduced water production. *PLoS One*. 2014; 9(7): e102218. <https://doi.org/10.1371/journal.pone.0102218> PMID: 25029447
17. Kleiner DE, Brunt EM, Van Natta M, Behling C, Contos MJ, Cummings OW, et al. Design and validation of a histological scoring system for nonalcoholic fatty liver disease. *Hepatology*. 2005; 41(6): 1313–1321. <https://doi.org/10.1002/hep.20701> PMID: 15915461
18. Sellmann C, Priebes J, Landmann M, Degen C, Engstler AJ, Jin CJ, et al. Diets rich in fructose, fat or fructose and fat alter intestinal barrier function and lead to the development of nonalcoholic fatty liver disease over time. *J Nutr Biochem*. 2015; 26(11): 1183–92. <https://doi.org/10.1016/j.jnutbio.2015.05.011> PMID: 26168700
19. Jin CJ, Engstler AJ, Sellmann C, Ziegenhardt D, Landmann M, Kanuri G, et al. Sodium butyrate protects mice from the development of the early signs of non-alcoholic fatty liver disease: role of melatonin and lipid peroxidation. *Br J Nutr*. 2016; 116(10): 1682–1693.
20. Sellmann C, Baumann A, Brandt A, Jin CJ, Nier A, Bergheim I. Oral Supplementation of Glutamine Attenuates the Progression of Nonalcoholic Steatohepatitis in C57BL/6J Mice. *J Nutr*. 2017; 147(11): 2041–2049. <https://doi.org/10.3945/jn.117.253815> PMID: 28931589
21. Peralta C, Bulbena O, Xaus C, Prats N, Cutrin JC, Poli G, et al. Ischemic preconditioning: a defense mechanism against the reactive oxygen species generated after hepatic ischemia reperfusion. *Transplantation*. 2002; 73(8): 1203–1211. <https://doi.org/10.1097/00007890-200204270-00004> PMID: 11981410

22. Nasuti C, Coman MM, Olek RA, Fiorini D, Verdenelli MC, Cecchini C, et al. Changes on fecal microbiota in rats exposed to permethrin during postnatal development. *Environ Sci Pollut Res Int*. 2016; 23(11): 10930–10937. <https://doi.org/10.1007/s11356-016-6297-x> PMID: 26898931
23. Milani C, Hevia A, Foroni E, Duranti S, Turroni F, Lugli GA et al. Assessing the fecal microbiota: an optimized ion torrent 16S rRNA gene-based analysis protocol. *PLoS One*. 2013; 8: e68739. <https://doi.org/10.1371/journal.pone.0068739> PMID: 23869230
24. Caporaso JG, Kuczynski J, Stombaugh J, Bittinger K, Bushman FD, Costello EK et al. QIIME allows analysis of high-throughput community sequencing data. *Nat Methods*. 2010; 7(5): 335–336. <https://doi.org/10.1038/nmeth.f.303> PMID: 20383131
25. Edgar RC. Search and clustering orders of magnitude faster than BLAST. *Bioinformatics*. 2010; 26: 2460–2461. <https://doi.org/10.1093/bioinformatics/btq461> PMID: 20709691
26. Quast C, Pruesse E, Yilmaz P, Gerken J, Schweer T, Yarza P, et al. The SILVA ribosomal RNA gene database project: improved data processing and web-based tools. *Nucleic Acids Res*. 2013; 41: D590–596. <https://doi.org/10.1093/nar/gks1219> PMID: 23193283
27. Zhu Y, Sun Y, Wang C, Li F. Impact of dietary fibre:starch ratio in shaping caecal archaea revealed in rabbits. *J Anim Physiol Anim Nutr (Berl)*. 2017; 101(4): 635–640.
28. Lozupone C, Knight R. UniFrac: a new phylogenetic method for comparing microbial communities. *Appl Environ Microbiol*. 2005; 71: 8228–8235. <https://doi.org/10.1128/AEM.71.12.8228-8235.2005> PMID: 16332807
29. La Mura V, Pasařin M, Rodriguez-Vilarrupla A, García-Pagán JC, Bosch J, Abalde JG. Liver sinusoidal endothelial dysfunction after LPS administration: a role for inducible-nitric oxide synthase. *J Hepatol*. 2014; 61(6): 1321–7. <https://doi.org/10.1016/j.jhep.2014.07.014> PMID: 25038487
30. Fujita K, Seike T, Yutsudo N, Ohno M, Yamada H, Yamaguchi H, et al. Hydrogen in drinking water reduces dopaminergic neuronal loss in the 1-methyl-4-phenyl-1,2,3,6-tetrahydropyridine mouse model of Parkinson's disease. *PLoS One*. 2009; 30(9): e7247.
31. Shin DW, Yoon H, Kim HS, Choi YJ, Shin CM, Park YS, et al. Effects of Alkaline-Reduced Drinking Water on Irritable Bowel Syndrome with Diarrhea: A Randomized Double-Blind, Placebo-Controlled Pilot Study. *Evid Based Complement Alternat Med*. 2018; 15. <https://doi.org/10.1155/2018/9147914> PMID: 29849734
32. Chang PV, Hao L, Offermanns S, Medzhitov R. The microbial metabolite butyrate regulates intestinal macrophage function via histone deacetylase inhibition. *Proc Natl Acad Sci U S A*. 2014; 111(6): 2247–52. <https://doi.org/10.1073/pnas.1322269111> PMID: 24390544
33. Kelly CJ, Zheng L, Campbell EL, Saeedi B, Scholz CC, Bayless AJ, et al. Crosstalk between Microbiota-Derived Short-Chain Fatty Acids and Intestinal Epithelial HIF Augments Tissue Barrier Function. *Cell Host Microbe*. 2015; 17(5): 662–71. <https://doi.org/10.1016/j.chom.2015.03.005> PMID: 25865369
34. Xiao X, Nakatsu G, Jin Y, Wong S, Yu J, Lau JY. Gut Microbiota Mediates Protection Against Enteropathy Induced by Indomethacin. *Sci Rep*. 2017; 7: 40317. <https://doi.org/10.1038/srep40317> PMID: 28067296
35. Rivière A, Selak M, Lantin D, Leroy F, De Vuyst L. Bifidobacteria and Butyrate-Producing Colon Bacteria: Importance and Strategies for Their Stimulation in the Human Gut. *Front Microbiol*. 2016; 7: 979. <https://doi.org/10.3389/fmicb.2016.00979> PMID: 27446020
36. Macfarlane S, Macfarlane GT. Regulation of short-chain fatty acid production. *Proc Nutr Soc*. 2003; 62(1): 67–72. <https://doi.org/10.1079/PNS2002207> PMID: 12740060
37. Million M, Raoult D. Linking gut redox to human microbiome. *Human Microbiome Journal*. 2018. <https://doi.org/10.1016/j.humic.2018.07.002>
38. Vorobjova NV. Selective stimulation of the growth of anaerobic microflora in the human intestinal tract by electrolyzed reducing water. *Med Hypotheses*. 2005; 64: 543–546. <https://doi.org/10.1016/j.mehy.2004.07.038> PMID: 15617863
39. Higashimura Y, Baba Y, Inoue R, Takagi T, Uchiyama K, Mizushima K, et al. Effects of molecular hydrogen-dissolved alkaline electrolyzed water on intestinal environment in mice. *Med Gas Res*. 2018; 8(1): 6–11. <https://doi.org/10.4103/2045-9912.229597> PMID: 29770190
40. Blachier F, Davila AM, Mimoun S, Benetti PH, Atanasiu C, Andriamihaja M, et al. Luminal sulfide and large intestine mucosa: friend or foe? *Amino Acids*. 2010; 39(2): 335–47. <https://doi.org/10.1007/s00726-009-0445-2> PMID: 20020161